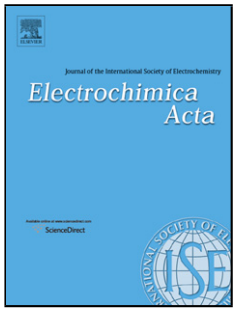

Title: Nanostructured electropolymerized poly(methylene blue) films from deep eutectic solvents. Optimization and characterization

Authors: Oana Hosu, Mădălina M. Bârsan, Cecilia Cristea, Robert Săndulescu, Christopher M.A. Brett

PII: S0013-4686(17)30421-8
DOI: http://dx.doi.org/doi:10.1016/j.electacta.2017.02.142
Reference: EA 29007

To appear in: *Electrochimica Acta*

Received date: 2-12-2016
Revised date: 24-2-2017
Accepted date: 26-2-2017

Please cite this article as: Oana Hosu, Mădălina M.Bârsan, Cecilia Cristea, Robert Săndulescu, Christopher M.A.Brett, Nanostructured electropolymerized poly(methylene blue) films from deep eutectic solvents.Optimization and characterization, Electrochimica Acta http://dx.doi.org/10.1016/j.electacta.2017.02.142

Nanostructured electropolymerized poly(methylene blue) films from deep eutectic solvents. Optimization and characterization

Oana Hosu[1,2], Mădălina M. Bârsan[1], Cecilia Cristea[2], Robert Săndulescu[2],

Christopher M.A. Brett[1*]

[1]*Department of Chemistry, Faculty of Sciences and Technology, University of Coimbra, 3004-535 Coimbra, Portugal*

[2]*Department of Analytical Chemistry, Faculty of Pharmacy, "Iuliu Haţieganu" University of Medicine and Pharmacy, 400349 Cluj-Napoca, Romania*

* Corresponding author:

Tel: +351-239854470
FAX: +351-239827703
e-mail: cbrett@ci.uc.pt

Graphical abstract

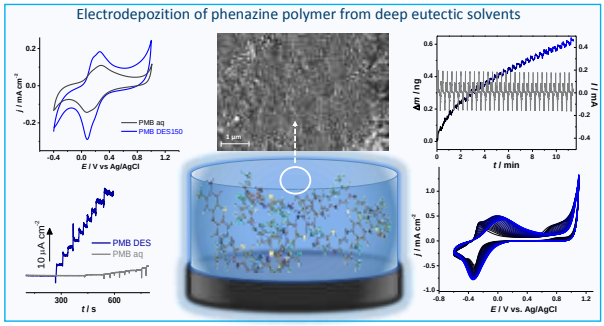

Highlights

- Deep eutectic solvents (DES) for the polymerization of methylene blue (MB)
- Polymerization method optimization by varying electrochemical parameters
- Electrochemical quartz crystal microbalance study of polymerization process
- Electrochemical and surface characterization of DES polymer modified electrodes
- Application of PMB_{DES} modified electrodes to the detection of ascorbate

Abstract

Electropolymerization in deep eutectic solvents (DES) as a new class of "green" solvents, was employed to prepare poly(methylene blue) (PMB) polymers with different nanostructured morphologies. PMB films were synthesized on glassy carbon electrodes by potential cycling from a mixture of 90% ethaline (choline chloride : ethylene glycol) and 10% aqueous solution with different ionic composition, i.e. Na^+, SO_4^{2-}, ClO_4^-, NO_3^-, Cl^-. The scan rate during polymerization was the key parameter in controlling film structure, confirmed by scanning electron microscopy. Electrochemical characterization of the polymers demonstrated differences in the electrochemical voltammetric and impedance properties of all synthesized PMB films. The PMB film obtained at 150 mV s^{-1} polymerisation scan rate with stirring, formed nanostructured ordered and granular films, was shown to have superior electrochemical properties. Electrochemical quartz crystal microbalance gravimetry was used to quantify the amount of deposited film and probe the polymerization mechanism. PMB film modified electrodes obtained in optimized DES media at different scan rates were tested for ascorbate sensing, in order to establish the most suitable PMB_{DES} film for (bio)sensing applications.

Keywords: nanostructured polymer film; poly(methylene blue); deep eutectic solvent; ethaline; electropolymerization; electrochemical sensor.

1. Introduction

The use of redox phenazine polymers has been shown to be efficient in many (bio)analytical applications, and methods to synthesize polymeric films with new nanostructured and controlled structures are still being investigated. Electrochemical methods prevail in the selective modification of electrodes, since they offer the possibility to tailor polymer structure by simply adjusting the electrochemical parameters [1]. Moreover, it has been shown that the medium used for the electrochemical synthesis of conducting/redox polymers has a strong influence on the structure, and therefore the properties of the obtained polymer films, especially the electronic conductivity [2, 3].

The use of deep eutectic solvents (DES) has emerged as an alternative in polymer synthesis and has shown to be successful in the preparation of advanced materials with controlled structure [4]. DES are molecular complexes, liquids at ambient temperature, formed between suitable hydrogen bond donors (HBD) and acceptors mixed in a specific mole ratio to enable the decrease of the resulting mixture's melting point, to a much lower temperature than that of the components. DES have the characteristics of ionic liquids, such as extended working temperature range, wide electrochemical window (important in electrochemical synthesis of polymers, which usually require the generation of radicals at high overpotential) and good chemical stability, but are easier to prepare, cost effective and biodegradable [4, 5]. Several nanomaterial syntheses have been reported in DES, namely shape-controlled nanoparticles, electrodeposited films, metal–organic frameworks, colloidal assemblies, hierarchically porous carbons, and DNA/RNA architectures, where DES can act as template, carbon or metal source and as reactant or auxiliary agent for synthetic processes [6]. Some DES parameters, such as viscosity, polarity, surface tension, can have a strong influence on the structure of the synthesized materials, mainly because of their control on species' reactivity and mass transport properties [6]. Recently, it has been shown that addition of water between 5 to 10 wt

% to DES improves their mass transport and conductivity characteristics. The addition of water introduces a second HBD and the relative interactions between the anion/cation and both HBDs will change the diffusion coefficients of each component [7, 8].

In electrochemistry, DES have been mostly employed for the electrodeposition of metals, alloys and semiconductors, in cases where the processes are difficult to achieve in aqueous solutions, since, due to hydrogen evolution, electrodeposition in water is generally limited [9-13]. The electrosynthesis of polymers in DES is still little explored; to the best of our knowledge only 5 papers report the use of DES for polymer electrosynthesis, i.e. for PEDOT [2, 14], PANI [3, 15], and recently for 3-aminophenylboronic acid, a derivative of aniline [16]. It was highlighted that the resulting polymers synthesized from DES had a higher electronic conductivity than their analogues synthesized in aqueous media.

This work describes for the first time the electrodeposition of the phenazine polymer poly(methylene blue) on glassy carbon electrodes (GCE), in solutions of methylene blue monomer dissolved in ethaline with 10% (v/v%) water content and different concentrations and ratios of ions, i.e. Na^+, SO_4^{2-}, ClO_4^-, NO_3^-, Cl^-. Polymers obtained in different DES media (PMB_{DES}) and at different scan rates from 50 to 500 mV s^{-1} (PMB_{DES}50-500) were synthesized and characterized in order to choose the best conditions for PMB film formation. Scanning electron microscopy (SEM) was used to identify the different nanostructured polymer films obtained in the optimized DES composition medium at different scan rates, their structures being correlated with the electrochemical properties observed by cyclic voltammetry (CV) and electrochemical impedance spectroscopy (EIS). A PMB film-modified electrode was also prepared in optimized aqueous medium for comparison purposes (PMB_{aq}). Electrochemical quartz crystal microbalance (EQCM) studies enabled the determination of the mass deposited during MB polymerization and the polymerization mechanism.

Application to ascorbate sensing, evidenced the polymer with best properties for use as (bio)sensors.

2. Experimental

2.1. Reagents and solutions

All reagents were of analytical grade and were used without further purification. Millipore Milli-Q nanopure water (resistivity≥18 MΩ cm) was used for the preparation of all solutions.

Methylene blue, choline chloride, ethylene glycol, L-ascorbic acid (AA), potassium chloride, hydrochloric acid (37%), nitric acid (65%), sodium hydroxide, dibasic potassium phosphate sodium tetraborate, sodium sulphate were purchased from Sigma Aldrich, Germany. Perchloric acid (70%), potassium chloride and monobasic sodium phosphate were obtained from Fluka, Switzerland.

For electrochemical sensing studies, the supporting electrolyte was 0.1 M KCl solution containing 5 mM HCl (pH ≈ 4). All experiments were carried out at room temperature (25±1 ^{o}C).

2.2 Instrumentation

Electrochemical experiments were performed in a three electrode cell, containing the glassy carbon electrode (GCE-geometric area 0.00785 cm^2) as working electrode, a Pt wire counter electrode and an Ag/AgCl (3.0 M KCl) reference electrode, using a potentiostat/galvanostat μ-Autolab system (Metrohm-Autolab, Netherlands). Before each use, the surface of the GCE was cleaned with diamond spray (1 Micron) and polishing paper (Kemet, UK).

EIS experiments were carried by using a potentiostat/galvanostat/ZRA, (Gamry Instruments, Reference 600). A root mean square (rms) perturbation of 10 mV was applied over the frequency range 65 kHz–0.1 Hz, with 10 frequency values per frequency decade.

An EQCM 10 M, Gamry Instruments, containing a graphite quartz crystal (QC) with 10 MHz central frequency was used for the gravimetric studies.

A scanning electron microscope (SEM) (JEOL, JSM-5310, Japan) was used to characterize the morphology of the different PMB films deposited on carbon film electrodes.

The pH measurements were carried out with a CRISON 2001 micro pH-meter (Crison Instruments SA, Barcelona, Spain).

2.3. Preparation of MB polymerization solution

Ethaline was obtained by mixing a quaternary ammonium salt (choline chloride) with a HBD (ethylene glycol) in a 1:2 molar ratio, heating to 60°C, following pre-treatment of the solid choline chloride by heating it up to 100 ºC to evaporate any water. After cooling down to room temperature, ethaline is ready to use for the preparation of the MB polymerization solution. MB was dissolved first in aqueous solution containing a mixture of NaOH and $HClO_4$ in different concentrations and ratios (see Table 1). Ethaline was added to this solution, so that the final concentration of monomer was 5 mM in a mixture of 10% v/v aqueous solution: 90 % v/v ethaline, which was thoroughly stirred and sonicated in the ultrasound bath.

A uniform and reproducible PMB_{DES} film was obtained by cycling for 30 scans in the potential range -0.6 – +1.2 V; different scan rates were investigated, between 50 to 500 mV s^{-1}, and the films obtained were designated as PMB_{DES}50-500. The polymerization was performed in a stirred solution, with a magnetic stirrer set at 450 rpm. For comparison purposes, PMB was also prepared in aqueous medium, in a solution containing 1 mM MB in 0.025 M $Na_2B_4O_7$ + 0.1 M Na_2SO_4 (pH 9.2), at a scan rate of 50 mV s^{-1}, as in [19].

2.4. Analysis of ascorbate

The analysis of ascorbate analysis was done in a 2 mL cell, the GCE/PMB_{DES} or GCE/PMB_{aq} acting as a working electrode. Aliquots of a 50 mM AA standard solution were added, under continuous magnetic stirring, the additions corresponding to 10 or 20 μM ascorbate in the final volume. The current was recorded at a fixed applied potential of 0.2 V vs Ag/AgCl.

Standard solutions of 10 mM ascorbic acid (AA) were freshly prepared and kept at 4 ºC in a refrigerator before use.

3. Results and discussion

3.1. Optimization of electropolymerization procedure

3.1.1. Optimization of DES solution composition

In the synthesis of electropolymerized polymer films, the content of dissolved monomer in the solution is a critical factor in the growth mechanism of the polymer, and therefore on its properties [17, 18]. While the use of a monomer solution that is too concentrated can lead to an inhomogeneous and disordered polymer structure, which can hinder electron transfer through the polymer network, a too dilute monomer solution can lead to the formation of very thin, ordered films with smaller anodic/cathodic peak currents. The content of MB in aqueous solution was found to be optimum at 1 mM [19], but since the rate of diffusion and mass transport in DES are different, various concentrations from 1 to 10 mM MB in ethaline were evaluated. Due to the fact that in pure ethaline the monomer is not very soluble, MB was first dissolved in 1 M NaOH aqueous solution, followed by the addition of ethaline and $HClO_4$, to finally obtain 10% v/v aqueous: 90 % ethaline with 0.1 M NaOH and 0.1 M $HClO_4$ in the final mixture. The choice of best monomer concentration was made considering the values of the anodic and cathodic peak currents at the PMB modified electrodes, measured in 0.1 M

KCl and 5 mM HCl aqueous solution, at 50 mV s^{-1} (results not shown). It was observed that there is a large, almost linear, increase in the peak current at PMB_{DES}/GCE up to 5 mM MB, above which it remained almost constant for the films obtained using 6 to 10 mM MB. On this basis, a 5 mM monomer concentration was chosen for further studies.

It was observed in a previous study on the polymerization of EDOT in DES, that the content of DES plays an important role in the polymerization process, especially in terms of the anion type and concentration [2]. Therefore, the second step in optimizing the procedure of MB polymerization from ethaline was to use different acids as anion sources, namely HCl, $HClO_4$, HNO_3 and H_2SO_4. The amount of NaOH necessary to dissolve MB was also varied. Cyclic voltammograms recorded in the presence of different acids are displayed in Figure 1, and as observed from the polymerization profiles, the use of HNO_3 was not favourable for polymer formation, while the other three acids led to the deposition of PMB. Polymerization occurs with the formation of radical cations, in one step at +0.76 V in HCl, and in two steps at +0.71 and +1.0 V vs Ag/Ag/Cl, in $HClO_4$. During polymerization, the anodic peak current (-0.26 V) of the monomer, decreases and shifts towards more positive values i.e. -0.11 V in HCl, and -0.06 V in $HClO_4$. The cathodic peak remains at the same potential, the current remaining nearly constant in HCl, and decreasing in $HClO_4$. The polymerization profile in H_2SO_4 was similar to that observed in $HClO_4$, with the difference of higher anodic currents corresponding to radical formation. Even though the increase in the anodic peak current was more evident for the PMB_{DES} film obtained in HCl, film stability was very poor, and it immediately detached itself from the electrode when testing in 0.1 M KCl + 5mM HCl.

Higher faradaic currents were recorded at PMB_{DES} films obtained in H_2SO_4 and $HClO_4$, and, therefore, different concentrations of these two acids in combination with different concentrations of NaOH were tried. The PMB_{DES} films obtained were tested in (0.1 M KCl + 5 mM HCl) aqueous solution, the corresponding total faradaic current, peak separation and

capacitance values from analysis of the CVs being shown in Table 1. As observed, the capacitance values, calculated in the non-faradaic region of the CVs, at +0.6 V vs Ag/AgCl, vary depending on the medium, probably due to differences in the polymer film structure. Comparing the values in Table 1, it can be seen that the use of a higher concentration of NaOH led to a substantial decrease in the anodic and cathodic peak currents. The lowest peak separation of only 38 mV was obtained for the PMB_{DES} film deposited in the presence of 0.1 M NaOH and 0.1 M $HClO_4$. This medium was therefore chosen for further polymerization studies.

3.1.2. Optimization of electropolymerization scan rate

The influence of the electropolymerization scan rate was investigated in the optimised DES medium and MB concentration, owing to its influence on the mass transport of monomer from bulk solution to the electrode surface. Polymerization carried out at slow scan rate, between 5 to 50 mV s^{-1}, were not very successful, the peak current attributed to polymer formation remaining lower than that of the monomer, see Figure 2a. At higher scan rates, the polymer peak currents begin to be higher than those of the monomer; in addition, stirring the solution further improves the polymerization rate, with even higher currents (Figure 2 b-d). Stirring leads to a higher monomer concentration in the vicinity of the electrode surface, in the rather viscous DES media.

Cyclic voltammograms recorded at GCE modified, with PMB_{DES} deposited at different scan rates, in (0.1 M KCl + 5 mM HCl) aqueous solution are displayed in Figures 3a and b, and the values of the corresponding anodic and cathodic peak currents are shown in Figure 3c. As observed in Figure 3a, the peak currents corresponding to polymer films obtained at scan rates from 50 to 150 mV s^{-1} increase linearly with the scan rate. The polymers $PMB_{DES}200$ and $PMB_{DES}250$ show similar CV profiles with slightly lower peak currents compared to

$PMB_{DES}150$; however, for scan rates higher than 300 mV s^{-1}, the peak current values decrease substantially. Figure 3c shows that $PMB_{DES}150$ had the highest peak currents, followed by PMB_{DES} obtained at 250, 200 and 100 mV s^{-1}. It is well known that scan rate influences the morphology of the electrodeposited films, since it controls both the diffusion rate from bulk solution to the electrode surface and also the rate of the electrode processes. Probably in 10% v/v aqueous solution: 90% v/v ethaline, at 150 mV s^{-1} there is optimum combination of fast electrode kinetics with sufficient monomer arriving from bulk solution that enables the formation of polymer morphologies with the best electrochemical properties (see Section 3.2).

Figure 3d shows CVs recorded at PMB_{aq} and $PMB_{DES}150$ films, and it can be clearly seen that the latter exhibits substantially higher faradaic currents, demonstrating the advantage in using DES for the synthesis of PMB. The same tendency was observed for the polymer PEDOT when formed by electropolymerisation in DES [2]. The increase in both faradaic and capacitive currents can be correlated with the formation of nanostructured films (see Section 3.2).

In order to further investigate the differences in the morphology and in the electrochemical behaviour of PMB_{DES} films, 3 types of film were further evaluated. These were the one made using the optimized polymerization scan rate of 150 mV s^{-1}, and those for the minimum and maximum studied values of 50 and 500 mV s^{-1}.

3.2. Scanning electron microscopy characterization

SEM images were recorded on carbon film electrodes modified with PMB films formed in aqueous media and in DES at scan rates 50, 150, and 500 mV s^{-1} (Figure 4) and reveal the nanostructured morphology. PMB formed in aqueous media forms a relatively smooth surface

structure, as seen in Figure 4a, with some irregularities, similar to those of other reported electrosynthesized phenazine films, where PMB_{aq} was deposited on ITO electrodes [1].

Unlike the polymer obtained in aqueous medium, the SEM images of polymer formed in DES all reveal spherical-type formations of different dimensions, their size being influenced by the electropolymerisation scan rate. For 50 mV s^{-1} formation scan rate (Figure 4b), the sphere-like structures were not as well-defined as for the highest scan rates, being rather flat with diameters between 160 and 300 nm and with the presence of some light spots of smaller dimension below 100 nm. For 150 mV s^{-1}, ordered nanostructures are seen with dimensions of ~ 40 nm up to ~70 nm diameter (Figure 4c). The image for films formed at the fastest scan rate of 500 mV s^{-1}, shows some cauliflower-growths, with the formation of spherical nanostructures, diameter varying from 50 to 160 nm (Figure 4d).

3.3. Electrochemical characterization of the PMB_{DES} films

3.3.1. Cyclic voltammetry

In order to investigate whether the electrochemical process is a diffusion controlled or surface confined process, CVs were recorded at PMB_{DES}50, 150 and 500, at scan rates between 25 and 150 mV s^{-1} in 0.1 M KCl + 5 mM HCl. As observed at lower scan rates, there are two oxidation and reduction peaks that overlap and become one at faster scan rates. This is probably due to the fact that the oxidation/reduction process occurs in two steps, the first one being an incomplete doping/dedoping of the polymer. It was found that for the PMB_{DES}50 both oxidation and reduction processes were controlled by the diffusion of counter ions, from bulk solution to the inside during reduction and out of the polymer film during the oxidation process respectively, as well as for PMB_{aq} films. In the case of PMB_{DES}150 and 500, the electrochemical process was surface confined (see Figure 5). This may be explained by the fact at 50 mV s^{-1}, the film is rather smooth (see SEM image in Figure 4b), while the

nanostructured porous films obtained at 150 and 500 mV s^{-1} (Figure 4 c, d), enable some electrolyte solution to be trapped inside the polymer film, so that sufficient cations are able to maintain neutrality during the redox process.

3.3.2 Electrochemical impedance spectroscopy

Electrochemical impedance spectroscopy was used to analyse the surface and interfacial characteristics of GCE modified with different PMB films obtained from DES at scan rates 50, 150 and 500 mV s^{-1} (PMB_{DES}50, 150, 500), and with PMB obtained in aqueous media (PMB_{aq}). The applied potentials were 0.0, 0.13 and 0.25 V vs Ag/AgCl, chosen from the cyclic voltammograms recorded at the modified electrodes, and are close to the reduction, midpoint and oxidation potentials of PMB. Spectra recorded at 0.0 and 0.13 V are very similar, the one recorded at 0.13 V being presented in Figure 6a, while the one at 0.25 V, which is only slightly different, is shown in Figure 6b. All spectra present a semicircle extended over the high and medium frequency region, which can be attributed to charge transfer processes at the vicinity of the GCE surface, and capacitive lines in the low frequency region, reflecting the polarization of the films. Similar spectra were obtained at phenazine modified electrodes [20-22]. The deposition of PMB polymer films leads to a decrease of the overall impedance value (results not shown). The spectra were fitted using an equivalent electrical circuit, Figure 6c, comprising a cell resistance, R_Ω, in series with a combination of a charge transfer resistance, R_1, in parallel with a double layer constant phase element (CPE_1) and in series with a second CPE element (CPE_2). Results obtained by fitting the spectra are presented in Table 2. The first CPE represents the charge separation at the electrode/polymer film while the second one comprises both the charge separation at the polymer/solution interface and the polarization of the polymer film. The CPE element is defined as CPE =

$[(Ci\omega)^{\alpha}]^{-1}$, a pure capacitor in the case of $\alpha = 1$ or as a non-ideal capacitor, due to the porosity and non-homogeneity of the surface, for $0.5 < \alpha < 1$.

As observed, the spectra in the high frequency region are very similar for all modified electrodes (at both applied potentials) the differences appearing only in the medium and low frequency region. This indicates that the charge separation processes occurring at the GCE/polymer interface are not significantly influenced by the polymer bulk structure, reflected by the similar values of CPE_1 for GCE modified with different PMB_{DES} films, with values between 0.9 and 1.4 mF cm^{-2} s^{a-1} at 0.13 V and slightly higher, between 1.3 and 3.1 mF cm^{-2} s^{a-1}, at 0.25 V, the highest value being for $PMB_{DES}150$. PMB_{aq} had only slightly smaller values of CPE_1 at both applied potentials. However, it is important to notice that α_1 values were very high for $PMB_{DES}150$, indicating the formation of a very homogeneous compact film on the electrode surface, which probably facilitates the charge transfer processes at the electrode/polymer interface, reflected by the low R_1 values (see Table 2).

The medium frequency part of the spectra began to differ according to the PMB_{DES} film, the polymer film structure having a stronger influence. The differences are more evident at 0.25 V vs Ag/AgCl, where R_1 was significantly lower (60 Ω cm^2) at $PMB_{DES}150$ than at the other two PMB films, which were 393 and 730 Ω cm^2 for $PMB_{DES}50$ and 500, respectively. At 0.13 V the R_1 values decreased in the order $PMB_{DES}500 > PMB_{DES}50 > PMB_{DES}150$, from 560 down to 196 Ω cm^2. The R_1 values obtained at GCE modified with PMB_{aq} were 3 orders of magnitude higher than those at GCE/PMB_{DES} (4.9 and 21 kΩ cm^2).

The values of CPE_2 were of the same magnitude as CPE_1 and slightly higher for $PMB_{DES}50$, than for $PMB_{DES}150$ and 500, which had similar values. PMB_{aq} exhibited the highest polarization capacitance, of 6.8 and 7.6 mF $cm^{-2}s^{a-1}$. However, the α_2 values were very small for PMB_{aq} (0.60), probably due to heterogeneity of the film, as also observed in the SEM

images. The highest value of α_2 was obtained at $PMB_{DES}500$, followed by $PMB_{DES}150$, films with similar nanostructure.

Thus, the EIS results indicate that $PMB_{DES}150$ forms a homogeneous compact structure on the electrode surface and the GCE/$PMB_{DES}150$ exhibits the lowest charge transfer resistance, only 60 Ω cm^2 at 0.25 V vs Ag/AgCl.

3.3.3 Electrochemical quartz crystal microbalance

The EQCM was used to monitor the electrodeposition process of PMB in DES, using the optimized procedure using 5 mM MB in 90 % ethaline with 10% v/v (0.1 M NaOH + 0.1 M $HClO_4$) aqueous solution, at v = 150 mV s^{-1}. For rigid films, the deposited mass can be determined using the Sauerbrey equation [23]:

$$\Delta f = -\frac{2 f_0^2}{A\sqrt{\mu_q \rho_q}} \Delta m$$

where f_0 is the resonant frequency (Hz), Δf the frequency change (Hz), Δm the mass change (g), A the piezoelectrically active crystal area, ρ_q the density of quartz (g cm^{-3}) and μ_q the shear modulus of quartz for AT-cut crystals (g cm^{-1} s^{-2}). The graphite QC conversion factor, $-\Delta f / \Delta m$, is thus 226.0 Hz μg^{-1}, or 1.104 Hz cm^{-2} ng^{-1}. The microbalance used in this work permits simultaneous recording of two resonant frequencies, in series and in parallel, which allows determination of the dissipation factor, which, if it varies, indicates formation of a viscoelastic film [24]. The dissipation factor did not vary which confirms the rigidity of the film (data not shown).

A typical gravimetric-electrochemical measurement is displayed in Figure 7a, which shows the mass variation together with both current and potential variation with time during potential scanning; the mass and current variation during one scan is shown in Figure 7b.

The overall polymerization process occurs in three steps during each polymerization cycle: the oxidation of monomer/polymer, the formation of radical cations and the reduction of monomer/polymer, which all have a different influence on the deposited mass.

The total deposited mass after 30 cycles is 685 ng, the increase in mass being depicted in Figure 7c. It can be observed that there is a sharp increase in the deposited mass during the first 4 polymerization cycles, of 213 ng, followed by another 120 ng up to the 10^{th} cycle. After the 10^{th} cycle the deposition rate decreases and becomes linear, with a mass increase of 14-18 ng per cycle, reaching 685 ng after the 30^{th} cycle. This is a typical polymerization process, which initiates with the formation of nucleation islands that then gradually grow and form a uniform layer, which corresponds to the first 10 cycles. After the formation of a uniform layer of polymer, its growth becomes linear, with a constant increase in polymer film thickness with each cycle, from 10 to 30 cycles. A different gravimetric profile was recorded when PMB_{aq} was deposited on AuQC and on graphite QC, when a small mass variation was observed during the initial 5 cycles, the main increase in mass beginning with the 15^{th} and 18^{th} cycle, respectively, up to the 30^{th} cycle [25].

The deposition of a larger amount of polymer during the first cycles is in agreement with the CV data, (Figure 2b), which shows that the production of radical cations occurs mainly in the first 10 potential cycles, since this process occurs better on graphite than on the polymer film, leading to a higher rate of PMB formation. Therefore, radical formation decreases upon formation of polymer islands and is almost not seen after full coverage of the graphite QC surface; the deposition of polymer afterwards probably occurs by the covalent linkage of the already formed short branches of polymer [25].

The amplification of Figure 7a (showed at the left for cycles 9-12) and Figure 7b, give examples of mass, current and potential variation with time and current and mass variation

upon potential cycling, respectively, applicable for cycles between 9-30, when the electrode surface is fully covered, as explained above. It can be observed that during the first 10 s of the cycle, between -0.6 and 0.8 V, the mass remains constant, followed by a slight decrease between 0.8 and 1.1 V of 12 ng owing to formation of radical cations. During the reverse scan, the mass increases, first slightly between 1.1 and 0.0 V, by 10 ng, and then more sharply for the last 4 s of the polymerization cycle, from 0.0 to -0.6 V, by 18 ng. The fact that the mass gain only occurs during the reverse scan, corresponding to the reduction process, can be explained taking into consideration two factors: i) the radical cations formed at positive potentials begin to react with each other during the reverse scan, forming oligomers on the electrode surface, and ii) during the reduction of the polymer there is insertion of cationic solvent molecules inside the polymer film, to maintain neutrality, which also leads to a mass increase [19]. This explains why the mass variation during the first 10 polymerization cycles does not follow the same trend, since mass variations due to counterion diffusion are still not evident, as there are only small islands of polymer on the electrode surface.

Considering the difference between the resonant frequency of the graphite QC before and after the deposition of PMB_{DES}, measured in aqueous 0.1 M KCl, the deposited mass was 582 ng. This means that 15% of the mass deposited during polymerization is lost after washing, being probably loosely bound oligomers and monomers trapped inside the polymer network.

Film stability was also evaluated by measuring both mass and current variation upon potential cycling from -0.4 to +0.6 V during 30 scans, at 50 mV s^{-1} (results not shown). Mass variation occurs during each cycle, correlated with counterion diffusion into and out of the polymer film. From the initial total mass of 582 ng, there was a mass loss of 40 ng, meaning that less than 7% of the mass is lost upon repeated cycling. Note that the majority of mass was lost during the first 10 scans. At the same time, there was a reduction of 10% of the initial current.

It can be concluded that $PMB_{DES}150$ films are sufficiently stable to be using for sensing purposes.

3.4. Application of PMB to ascorbate sensing

In order to compare the analytical properties of the GCE modified with different PMB films obtained from DES at scan rates between 100 and 500 mVs^{-1}, and with PMB_{aq}, they were tested for the detection of the model analyte ascorbate, using fixed potential amperometry, at +0.2 V vs. Ag/AgCl. Typical chronamperograms at GCE modified with $PMB_{DES}150$ and PMB_{aq}, are displayed in Figure 8a, where it can be clearly seen that the sensors based on PMB_{DES} exhibited a significantly higher sensitivity towards ascorbate oxidation. The calibration plots of all tested modified electrodes are shown in Figure 8b with the corresponding analytical parameters in Table 3. As observed, the highest sensitivity of 350 ± 17 µA cm^{-2} mM^{-1} (RSD = 4.8%, *n*=3), and lowest detection limit, LOD = 3.6±0.4 µM (RSD = 11%, *n*=3), were recorded at GCE/$PMB_{DES}150$, only slightly superior to that of $PMB_{DES}100$ and $PMB_{DES}200$. The sensor with lowest sensitivity was that based on $PMB_{DES}500$. Thus, $PMB_{DES}150$ appears to be the most suitable for sensing applications.

4. Conclusions

PMB polymer films with unique nanostructures have been successfully synthesized in ethaline plus 10% v/v aqueous solution of 0.1 M NaOH and 0.1 M $HClO_4$ in the final DES optimised mixture. The scan rate used during electropolymerization was a crucial factor in influencing the structure and morphology, and thence the electrochemical properties of the resulting PMB_{DES} films. Comparison with PMB_{aq} revealed that all PMB films obtained from DES exhibited higher redox currents and a significantly lower charge transfer resistance than PMB_{aq}. Among the PMB_{DES} films analyzed, the highly ordered nanoparticles observed in the

SEM images at $PMB_{DES}150$ can be correlated with its superior electrochemical properties, namely the polymer faradaic currents and lowest charge transfer resistance. Gravimetric studies showed a total mass of PMB deposited on graphite QC electrodes of 685 ng, 15% being lost after polymer washing and only less than 7% upon repeated potential cycling. Moreover, GCE modified with PMB_{DES} obtained at different scan rates, from 100 to 500 mV s^{-1}, revealed their superior sensing performance compared to GCE/PMB_{aq}, and that $PMB_{DES}150$ is the most suitable for this purpose.

Acknowledgements

The authors are grateful for financial support from the Romanian National Authority for Scientific Research, CNCS - UEFISCDI, project number PNII-RU-TE-2014-4-0460 and from the Fundação para a Ciência e a Tecnologia (FCT), Portugal projects PTDC/QEQ-QAN/2201/2014, in the framework of Project 3599-PPCDT, and UID/EMS/00285/2013 (both co-financed by the European Community Fund FEDER), for financial support. O.H. thanks UMF for the internal grant number 7690/56/15.04.2016. M.M.B. thanks FCT for a postdoctoral fellowship SFRH/BPD/72656/2010.

References

[1] M.M. Bârsan, M.E. Ghica, C.M.A. Brett, Electrochemical sensors and biosensors based on redox polymer/carbon nanotube modified electrodes: a review, Anal Chim Acta, 881 (2015) 1-23.

[2] K.P. Prathish, R.C. Carvalho, C.M.A. Brett, Electrochemical characterisation of poly(3,4-ethylenedioxythiophene) film modified glassy carbon electrodes prepared in deep eutectic solvents for simultaneous sensing of biomarkers, Electrochim. Acta, 187 (2016) 704–713.

[3] P.M.V. Fernandes, J.M. Campiña, C.M. Pereira, F. Silva, Electrosynthesis of polyaniline from choline-based deep eutectic solvents: morphology, stability and electrochromism, J. Electrochem. Soc., 159 (2012) G97-G105 .

[4] F. del Monte, D. Carriazo, M.C. Serrano, M.C. Gutiérrez, M.L. Ferrer, Deep eutectic solvents in polymerizations: a greener alternative to conventional syntheses, ChemSusChem, 7 (2014) 999 – 1009.

[5] A. Paiva, R. Craveiro, I. Aroso, M. Martins, R.L. Reis, A.R.C. Duarte, Natural deep eutectic solvents − solvents for the 21st century, ACS Sustainable Chem. Eng., 2 (2014) 1063–1071.

[6] D.V. Wagle, H. Zhao, G.A. Baker, Deep eutectic solvents: sustainable media for nanoscale and functional materials, Acc. Chem. Res., 47 (2014) 2299−2308.

[7] A.P. Abbott, G. Frisch, K.S. Ryder, Electroplating using ionic liquids, Annu. Rev. Mater. Res., 43 (2013) 335–358.

[8] C. D'Agostino, L.F. Gladden, M.D. Mantle, A.P. Abbott, E.I. Ahmed, A.Y. Al-Murshedi, R.C. Harris, Molecular and ionic diffusion in aqueous – deep eutectic solvent mixtures: probing inter-molecular interactions using PFG NMR, Phys. Chem. Chem. Phys., 17 (2015) 15297-15304.

[9] A. Cojocaru, M.L. Mareş, P. Prioteasa, L. Anicăi, T. Vişan, Study of electrode processes and deposition of cobalt thin films from ionic liquid analogues based on choline chloride, J. Solid State Electrochem., 19 (2015) 1001-1014.

[10] Q.B. Zhang, A.P. Abbott, C. Yang, Electrochemical fabrication of nanoporous copper films in choline chloride-urea deep eutectic solvent, Phys. Chem. Chem. Phys., 17 (2015) 14702-14709.

[11] H. Yang, R.G. Reddy, Electrochemical deposition of zinc from zinc oxide in 2:1 urea/choline chloride ionic liquid, Electrochim. Acta, 147 (2014) 513-519.

[12] A.C. Wright, M.K. Faulkner, R.C. Harris, A. Goddard, A.P. Abbott, Nanomagnetic domains of chromium deposited on vertically aligned carbon nanotubes. J. Magn. Magn. Mater., 324 (2012) 4170− 4174.

[13] A.P. Abbott, J.C. Barron, G. Frisch, K.S. Ryder, A.F. Silva, The effect of additives on zinc electrodeposition from deep eutectic solvents, Electrochim. Acta, 56 (2011) 5272−5279.

[14] K.P. Prathish, R.C. Carvalho, C.M.A. Brett, Highly sensitive poly(3,4-ethylenedioxythiophene) modified electrodes by electropolymerisation in deep eutectic solvents, Electrochem. Commun., 44 (2014) 8-11.

[15] P.M.V. Fernandes, J.M. Campiña, N.M. Pereira, C.M. Pereira, F. Silva, Biodegradable deep eutectic mixtures as electrolytes for the electrochemical synthesis of conducting polymers, J. Appl. Electrochem., 42 (2012) 997–1003.

[16] F. Wang, F. Zou, X. Yu, Z. Feng, N. Du, Y. Zhong, X. Huang, Electrochemical synthesis of poly(3-aminophenylboronic acid) in ethylene glycol without exogenous protons, Phys. Chem. Chem. Phys., 18 (2016) 9999-10004.

[17] M.E. Ghica, C.M.A. Brett, Poly(brilliant cresyl blue) modified glassy carbon electrodes: Electrosynthesis, characterisation and application in biosensors, J. Electroanal. Chem., 629 (2009) 35–42.

[18] G. Zhang, A. Zhang, X. Liu, S. Zhao, J. Zhang, J. Lu, Investigation of the electropolymerization of o-toluldine and p-phenylenediamine and their electrocopolymerization by in situ ultraviolet-visible spectroelectrochemistry, J. Appl. Polym. Sci., 115 (2010) 2635-2647.

[19] M.M. Bârsan, E.M. Pinto, C.M.A Brett, Electrosynthesis and electrochemical characterization of phenazine polymers for application in biosensors, Electrochim. Acta, 53 (2008) 973-3982.

[20] S. Kakhki, M.M. Bârsan, E. Shams, C. M.A. Brett, Development and characterization of poly(3,4-ethylenedioxythiophene)-coated poly(methylene blue)-modified carbon electrodes, Synth. Met., 161 (2012) 2718-2726.

[21] M.M. Bârsan, C.T. Toledo, C.M.A. Brett, New electrode architectures based on poly(methylene green) and functionalized carbon nanotubes: Characterization and application to detection of acetaminophen and pyridoxine, J. Electroanal. Chem., 736 (2015) 8-15.

[22] V. Pifferi, M.M. Bârsan, M.E. Ghica, L. Falciola, C.M.A. Brett, Synthesis, characterization and influence of poly(brilliant green) on the performance of different electrode architectures based on carbon nanotubes and poly(3,4-ethylenedioxythiophene), Electrochim. Acta, 98 (2013) 199-207.

[23] G. Sauerbrey, Verwendung von Schwingquarzen zur Wägung dünner Schichten und zur Mikrowägung, Z. Phys., 155 (1959) 206-222.

[24] M.C. Dixon, Quartz crystal microbalance with dissipation monitoring: enabling real-time characterization of biological materials and their interactions, J. Biomol. Tech., 19(2008) 151–158.

[25] M.M. Bârsan, E.M. Pinto, C.M.A Brett, Methylene blue and neutral red electropolymerization on AuQCM and on modified AuQCM electrodes: an electrochemical and gravimetric study, Phys. Chem. Chem. Phys., 13 (2011) 5462-5471.

Tables

Table 1. Values of total faradaic current, peak separation and capacitance values (at +0.6 V) obtained from CVs recorded in (0.1 M KCl + 5 mM HCl) aqueous solution at 50 mV s^{-1} at GCE modified with PMB_{DES} obtained in ethaline with different concentrations of NaOH, $HClO_4$ and H_2SO_4 in a final mixture of 10% aqueous solution : 90% ethaline.

Acid	[acid] / M	[NaOH] / M	I_{pa} / µA cm^{-2}	I_{pc} / µA cm^{-2}	ΔE_p / mV	C / µF cm^{-2}
$HClO_4$	0.1	0.1	19.0	21.5	38	665
	0.2	0.1	9.7	7.4	50	912
	0.3	0.1	12.0	10.4	61	448
	0.1	0.25	9.6	9.4	66	876
	0.1	0.4	10.8	10.8	61	1065
H_2SO_4	0.1	0.1	10.8	9.4	52	678
	0.2	0.1	10.3	10.8	66	576
	0.3	0.1	14.6	10.7	72	927
	0.1	0.25	9.6	9.9	89	836
	0.1	0.4	8.4	10.4	61	955

Table 2. Values of equivalent circuit elements obtained by fitting the spectra in Figure 6.

Polymer	E / V vs. Ag/ AgCl	R_1 / Ω cm^2	CPE$_1$ / mF cm^{-2} s^{a-1}	a_1	CPE$_2$ / mF cm^{-2}s^{a-1}	a_2
$PMB_{DES}50$	0.13	268	1.41	0.84	1.35	0.74
	0.25	393	2.47	0.84	1.77	0.65
$PMB_{DES}150$	0.13	196	1.12	0.90	0.64	0.75
	0.25	60.0	3.12	1.00	1.03	0.72
$PMB_{DES}500$	0.13	560	0.95	0.73	0.51	0.86
	0.25	730	1.60	0.68	0.88	0.86
PMB_{aq}	0.13	21e3	0.90	0.79	7.60	0.60
	0.25	4.9e3	1.32	0.79	6.80	0.60

Table 3. Values of sensitivity and detection limits extracted from the calibration curves in Figure 8b obtained at GCE modified with PMB_{DES} electropolymerized at different scan rates and with PMB_{aq} (RSD < 5%, n = 3).

Polymer	Sensitivity / µA cm^{-2} mM^{-1}	LOD / µM
$PMB_{DES}100$	317	6.6
$PMB_{DES}150$	350	3.6
$PMB_{DES}200$	319	8.6
$PMB_{DES}300$	273	8.7
$PMB_{DES}400$	202	7.6
$PMB_{DES}500$	73	13.0
PMB_{aq}	23	7.8

Figure Captions

Figure 1. CVs recorded during polymerization of MB in a solution containing 5 mM MB in ethaline containing 0.1 M NaOH and 0.1 M of different acids at 50 mV s^{-1} (no stirring) a) HCl, b) $HClO_4$, c) HNO_3 and d) H_2SO_4; e) CVs at the different PMB films obtained in a-d at 50 mV s^{-1} in (0.1 M KCl + 5 mM HCl) aqueous solution.

Figure 2. CVs recorded during MB polymerization on GCE in a solution containing 5 mM MB in ethaline + (0.1 M NaOH + 0.1 M $HClO_4$) aqueous solution at different scan rates of a) 50, b) 150, c) 300 and d) 500 mV s^{-1} (with stirring).

Figure 3. CVs in (0.1 M KCl + 5 mM HCl) aqueous solution at GCE modified with PMB_{DES} obtained by electropolymerization at scan rates a) 50-150 mV s^{-1} and b) 150-500 mV s^{-1}; c) plot of peak current vs. polymerization scan rate; d) CVs at $PMB_{DES}150$ and PMB_{aq}; ν = 50 mV s^{-1}.

Figure 4. SEM images of films of a) PMB_{aq}, b) $PMB_{DES}50$, c) $PMB_{DES}150$ and d) $PMB_{DES}500$.

Figure 5. a) CVs in (0.1 M KCl + 5 mM HCl) aqueous solution at GCE/$PMB_{DES}150$ at rates 25-150 mV s^{-1} and b) plot of peak current versus scan rate.

Figure 6. Complex plane impedance plots in the frequency range 65 kHz - 0.1 Hz at GCE modified with PMB_{DES} formed by electropolymerization at different scan rates and with PMB_{aq} in (0.1 M KCl + 5 mM HCl) aqueous solution at a) 0.13 V and b) 0.25 V vs Ag/AgCl; c) equivalent circuit used to fit the spectra.

Figure 7. EQCM study of $PMB_{DES}150$ electrodeposition a) ─ mass, ─ current and --- potential variation during MB polymerization (on the right a magnification for cycles 9-12), b) mass and current change upon potential cycling during one scan and c) plot of mass deposited during each polymerization cycle.

Figure 8. a) Fixed potential chronoamperograms for oxidation of ascorbate for sequential additions of 10 μM ascorbate, at GCE modified with $PMB_{DES}150$ and PMB_{aq} in 0.1 M KCl; applied potential 0.2 V vs Ag/AgCl; b) calibration plots for ascorbate oxidation at GCE modified with PMB_{DES} electropolymerized at scan rates between 100 and 500 mV s^{-1}.

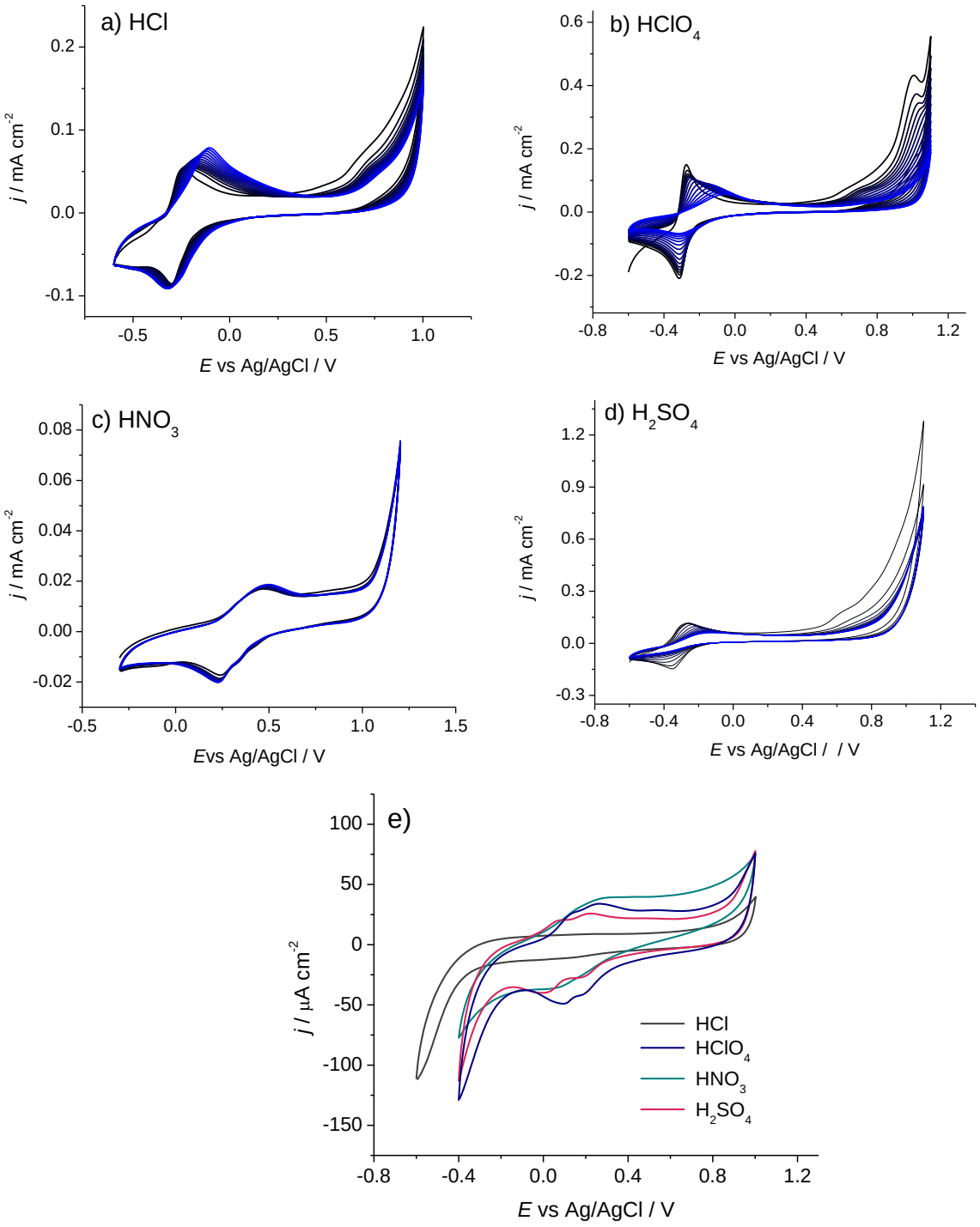

Figure 1. CVs recorded during polymerization of MB in a solution containing 5 mM MB in ethaline containing 0.1 M NaOH and 0.1 M of different acids at 50 mV s^{-1} (no stirring) a) HCl, b) $HClO_4$, c) HNO_3 and d) H_2SO_4, e) CVs recorded at the different PMB films obtained in a-d; e) CVs recorded at different PMB_{DES} obtained in a-d at 50 mV s^{-1} in (0.1 M KCl + 5 mM HCl) aqueous solution.

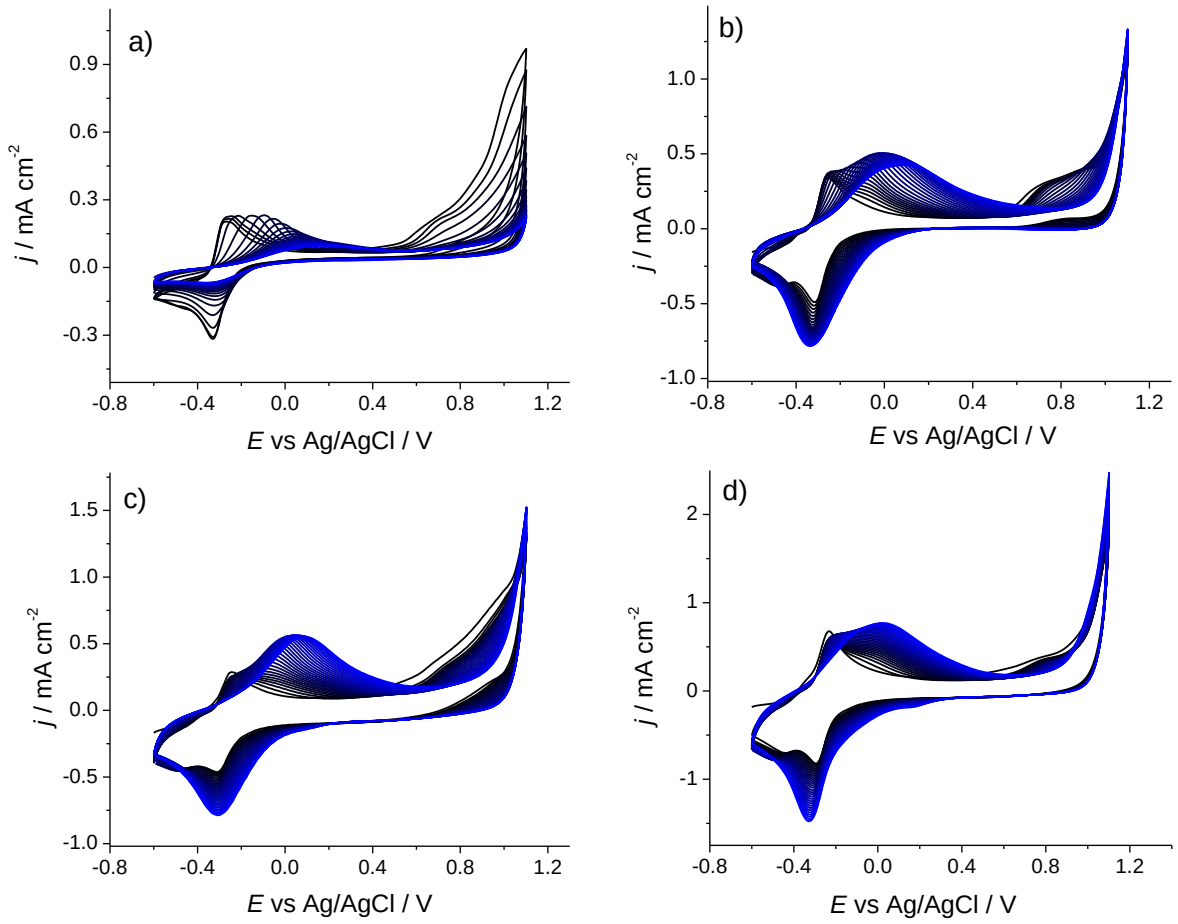

Figure 2. CVs recorded during MB polymerization on GCE in a solution containing 5 mM MB in ethaline + (0.1 M NaOH + 0.1 M $HClO_4$) aqueous solution at different scan rates of a) 50, b) 150, c) 300 and d) 500 mV s^{-1} (with stirring).

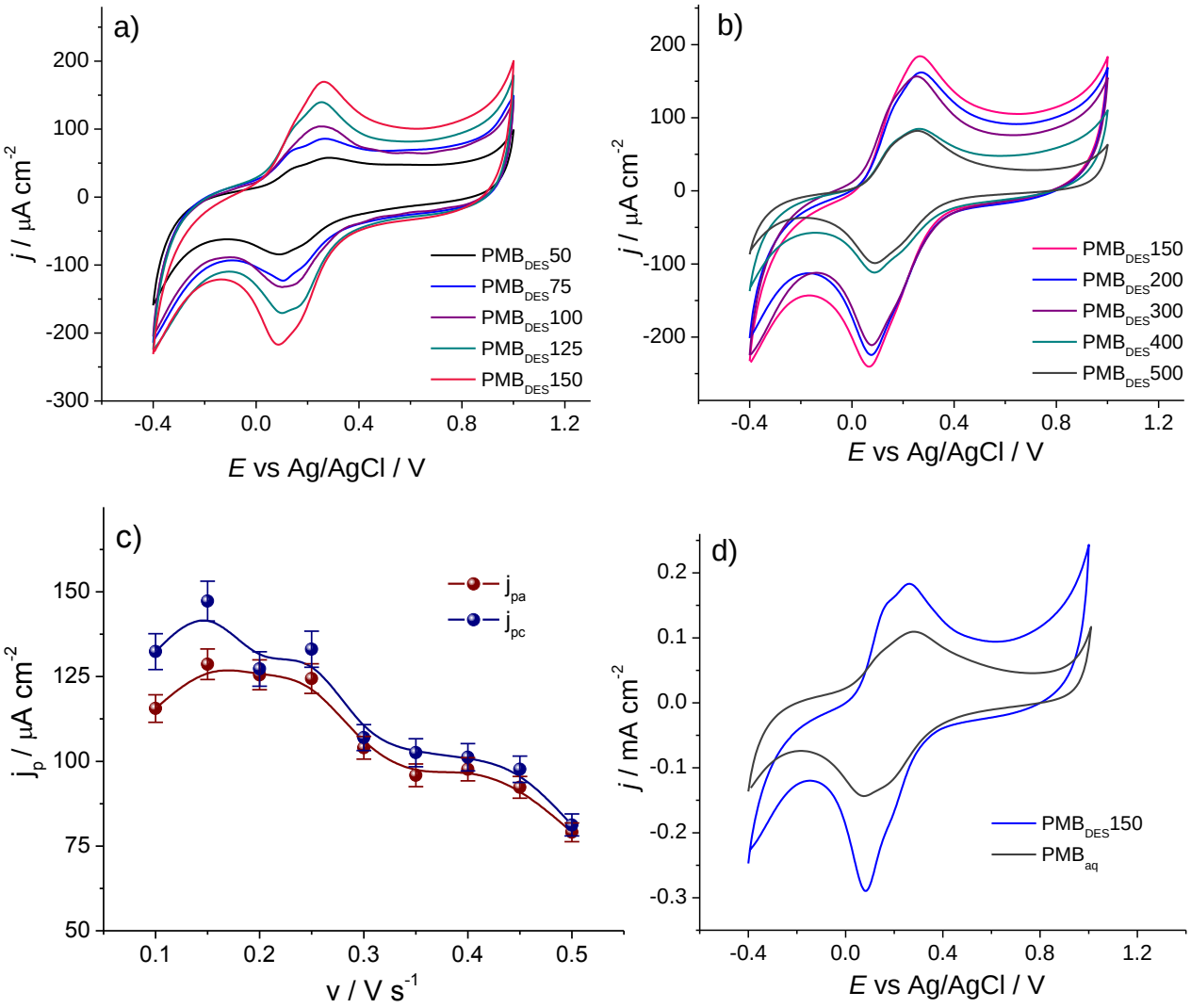

Figure 3. CVs in (0.1 M KCl + 5 mM HCl) aqueous solution at GCE modified with PMB_{DES} obtained by electropolymerization at scan rates a) 50-150 mV s^{-1} and b) 150-500 mV s^{-1};
c) plot of peak current vs. polymerization scan rate;
d) CVs at $PMB_{DES}150$ and PMB_{aq} (v = 50 mV s^{-1}).

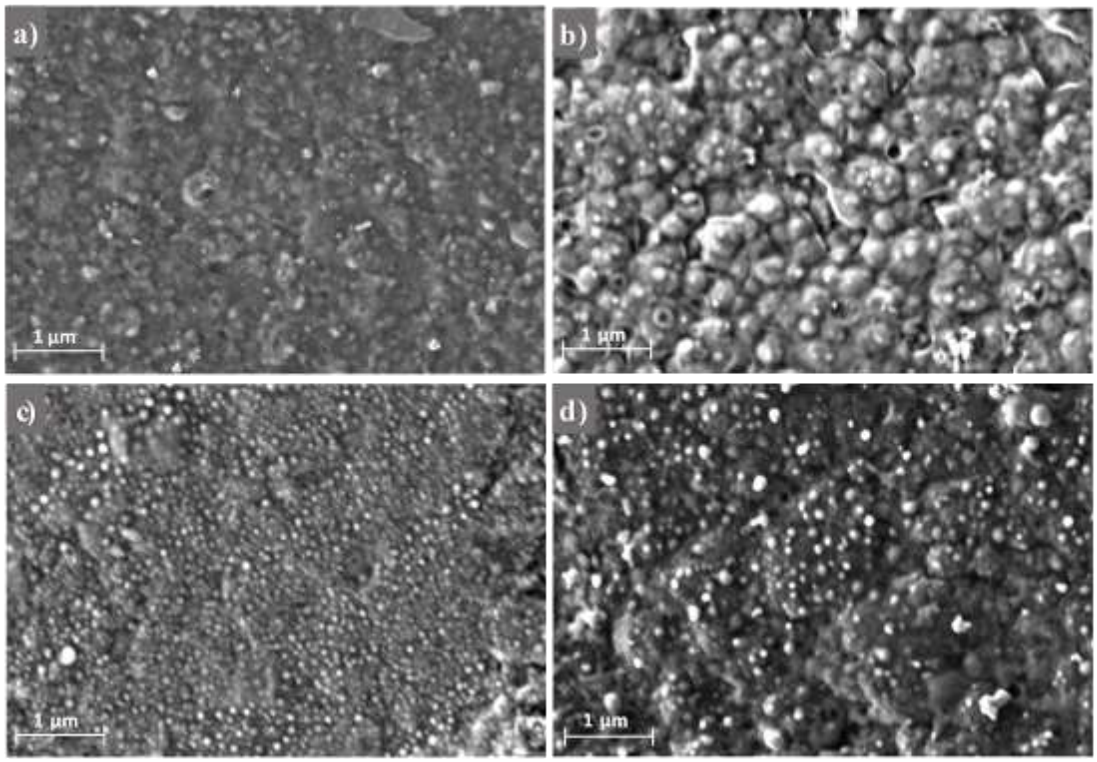

Figure 4. SEM images of films of a) PMB_{aq}, b) $PMB_{DES}50$, c) $PMB_{DES}150$ and d) $PMB_{DES}500$.

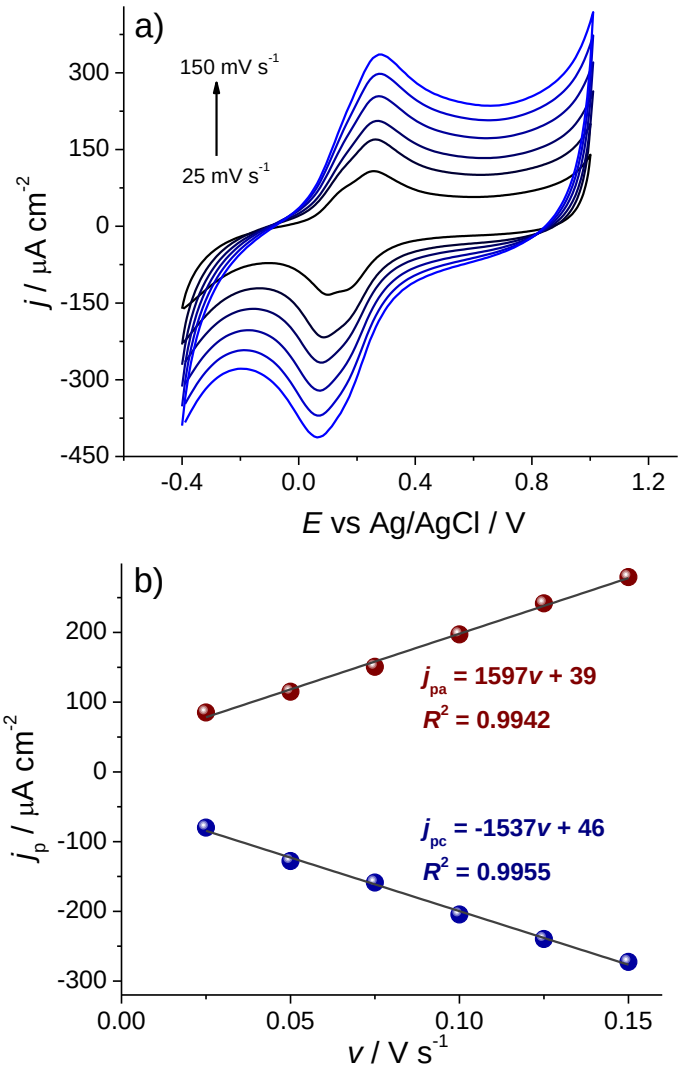

Figure 5. a) CVs in (0.1 M KCl + 5 mM HCl) aqueous solution at GCE/PMB_{DES}150 at rates 25-150 mV s^{-1} and b) plot of peak current versus scan rate.

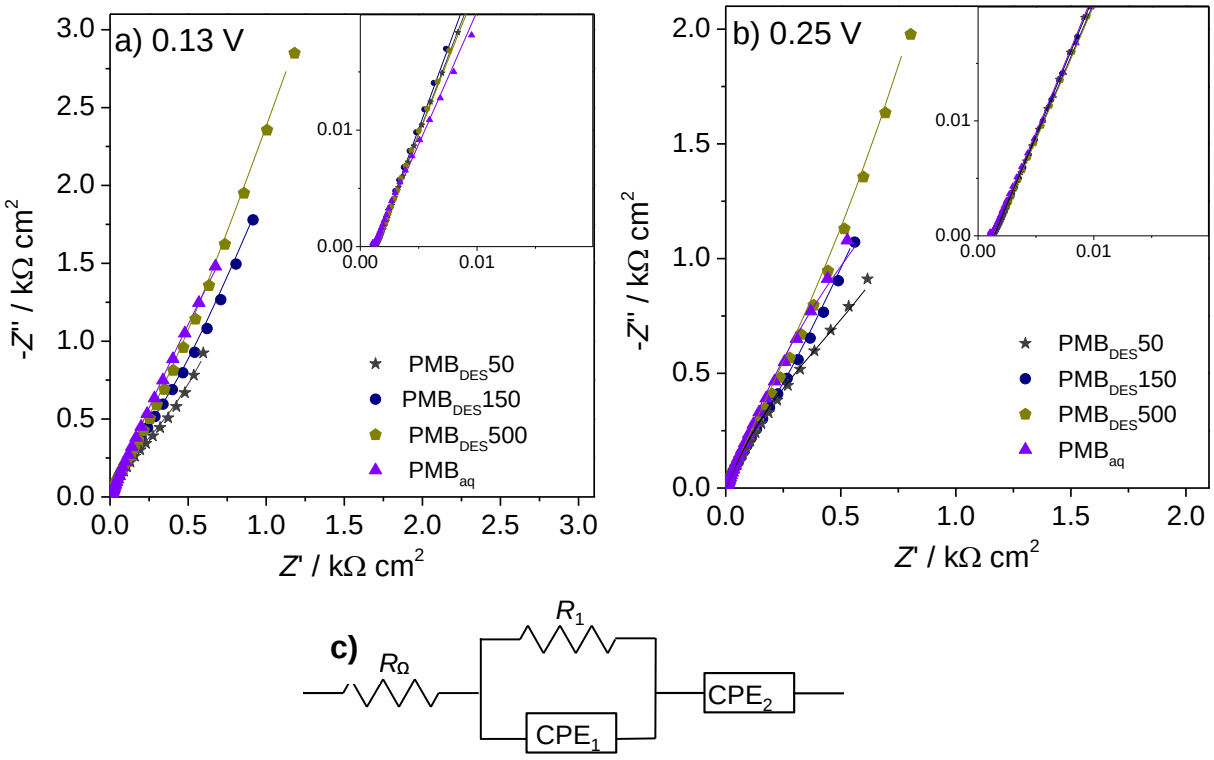

Figure 6. Complex plane impedance plots in the frequency range 65 kHz - 0.1 Hz at GCE modified with PMB_{DES} formed by electropolymerization at different scan rates and with PMB_{aq} in (0.1 M KCl + 5 mM HCl) aqueous solution at a) 0.13 V and b) 0.25 V vs Ag/AgCl; c) equivalent circuit used to fit the spectra.

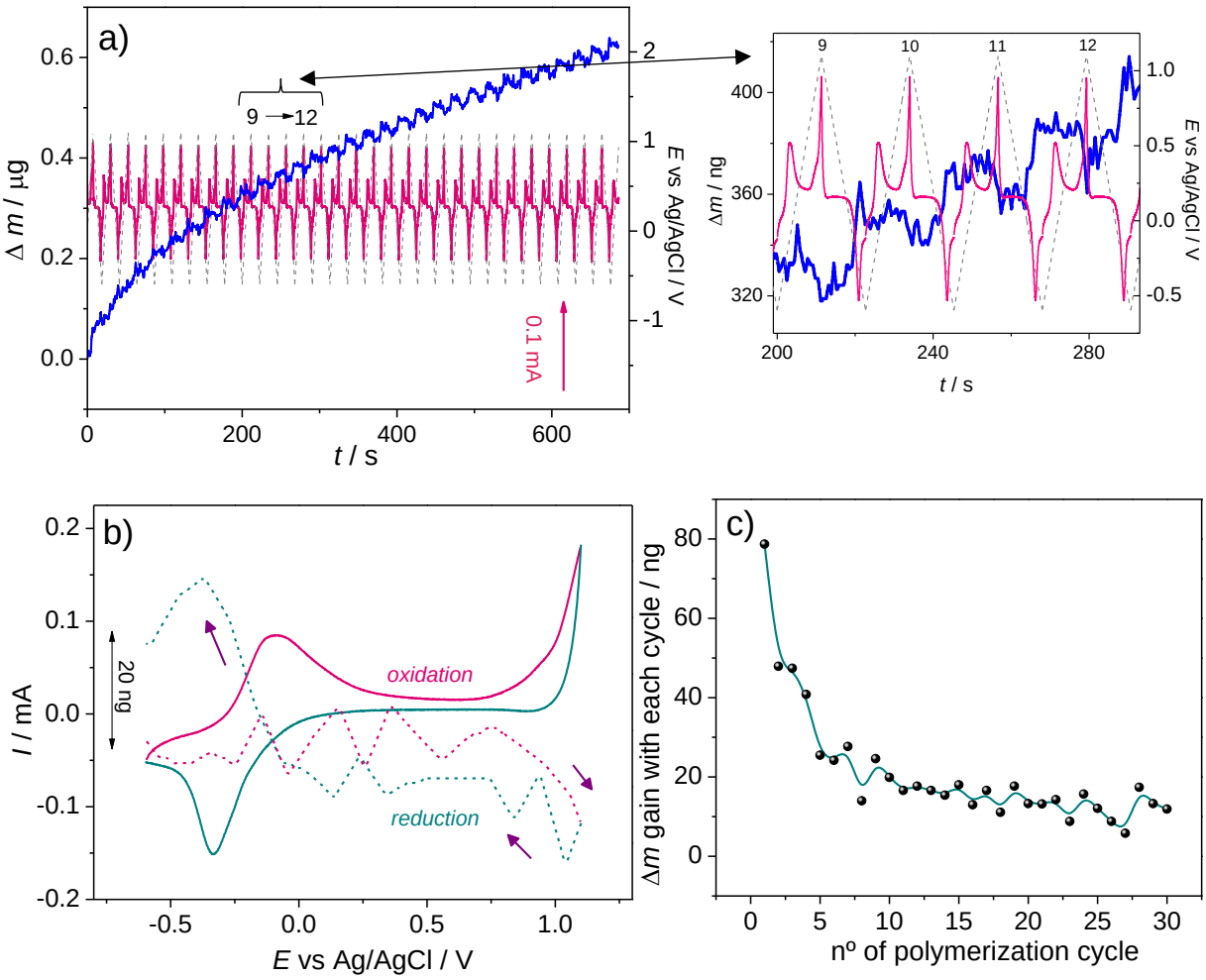

Figure 7. EQCM study of $PMB_{DES}150$ electrodeposition a) ─ mass, ─ current and --- potential variation during MB polymerization (on the right a magnification for cycles 9-12), b) mass and current change upon potential cycling during one scan and c) plot of mass deposited during each polymerization cycle.

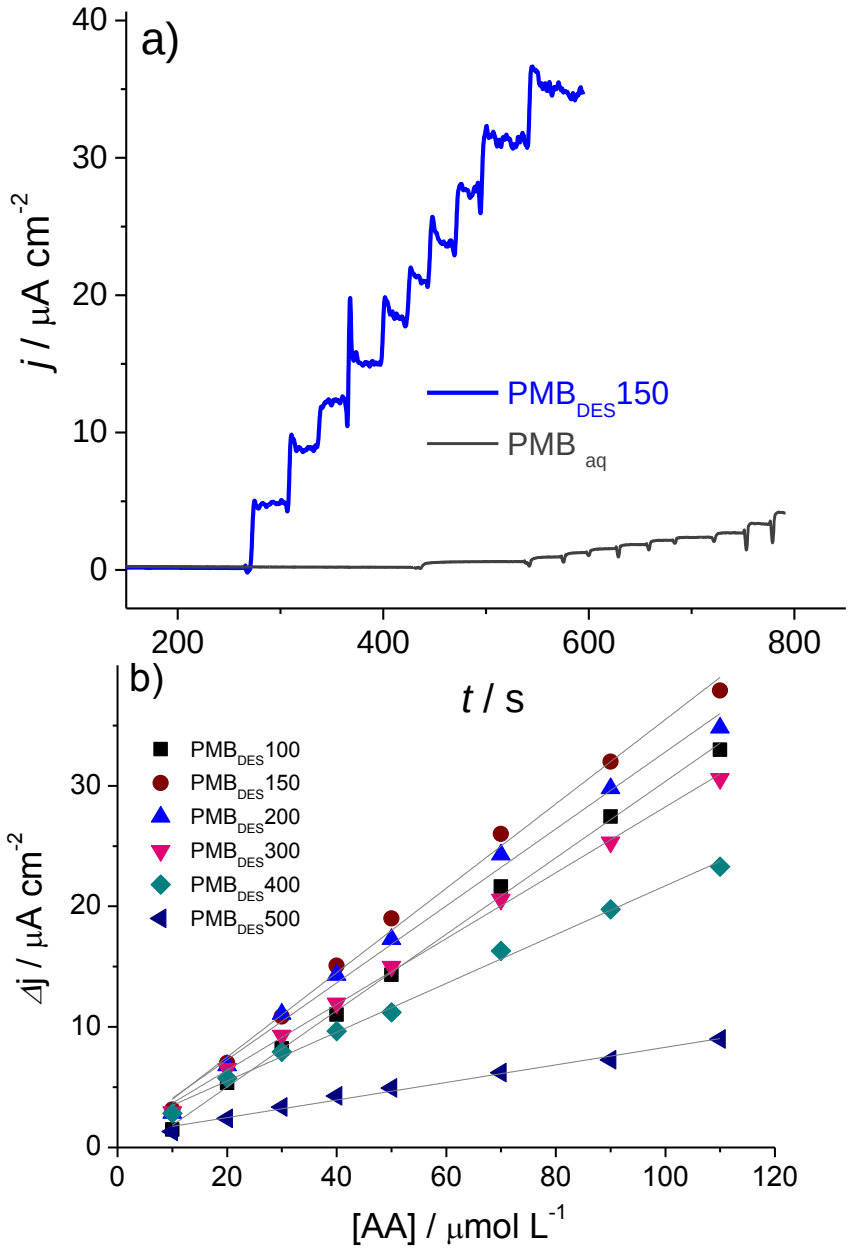

Figure 8. a) Fixed potential chronoamperograms for oxidation of ascorbate for sequential additions of ascorbate, at GCE modified with $PMB_{DES}150$ and PMB_{aq} in 0.1 M KCl; applied potential 0.2 V vs Ag/AgCl; b) calibration plots for ascorbate oxidation at GCE modified with PMB_{DES} electropolymerized at scan rates between 100 and 500 mV s^{-1}.